

Dual Lagrangian Learning for Conic Optimization

Mathieu Tanneau^{1,2} Pascal Van Hentenryck^{1,2}

Abstract

This paper presents Dual Lagrangian Learning (DLL), a principled learning methodology that combines conic duality theory with the representation power of ML models. DLL leverages conic duality to provide dual-feasible solutions, and therefore valid Lagrangian dual bounds, for parametric linear and nonlinear conic optimization problems. The paper introduces differentiable conic projection layers, a systematic dual completion procedure, and a self-supervised learning framework. The effectiveness of DLL is demonstrated on linear and nonlinear parametric optimization problems for which DLL provides valid dual bounds within 0.5% of optimality.

1. Introduction

From power systems and manufacturing to supply chain management, logistics and healthcare, optimization technology underlies most aspects of the economy and society. Over recent years, the substantial achievements of Machine Learning (ML) technology has spurred significant interest in combining the two methodologies. This integration has led to the development of new optimization algorithms (and the revival of old ones) taylored to ML problems, as well as new ML techniques for improving the resolution of hard optimization problems (Bengio et al., 2021). This paper focuses on the latter (ML for optimization), specifically, the development of so-called *optimization proxies*, i.e., ML models that provide approximate solutions to parametric optimization problems, see e.g., (Kotary et al., 2021).

In that context, considerable progress has been made in predicting *primal* solutions for a broad range of problems, from linear to discrete and nonlinear, non-convex optimization problems. State-of-the-art methods can now provide high-quality, feasible or close-to-feasible solutions (Chen et al.,

¹NSF AI Institute in Artificial Intelligence for Advances in Optimization ²H. Milton Stewart School of Industrial and Systems Engineering, Georgia Institute of Technology, Atlanta, USA. Correspondence to: Mathieu Tanneau <mathieu.tanneau@isye.gatech.edu>.

2023; Donti et al., 2021) for various applications (Kotary et al., 2021). In comparison, the task of predicting *dual* solutions has seldom received any attention in the literature. In particular, and despite the fundamental importance of duality theory in optimization, there is no unified framework for dual optimization proxies.

The paper addresses this gap by proposing Dual Lagrangian Learning (DLL), a principled learning methodology that combines conic duality theory with the representation power of ML models. DLL leverages conic duality to provide valid Lagrangian dual bounds for parametric linear and nonlinear conic optimization problems.

1.1. Related works

The vast majority of existing literature on optimization proxies focuses on predicting *primal* solutions and, especially, on ensuring their feasibility. This includes, for instance, physics-informed training loss (Fioretto et al., 2020; Pan et al., 2020; Donti et al., 2021), mimicking the steps of an optimization algorithm (Park & Van Hentenryck, 2023; Qian et al., 2023), using masking operations (Bello et al., 2016; Khalil et al., 2017), or designing custom projections and feasibility layers (Chen et al., 2023; Tordesillas et al., 2023). A key difference of DLL, besides the fact that it predicts a dual solution, is that it exploits the structure of the dual conic problem to design a general dual completion procedure, thus guaranteeing dual feasibility and removing the need for feasibility-focused techniques.

To the authors' knowledge, dual predictions have received very little attention, with most works using them to warm-start an optimization algorithm. A primal-dual prediction is used in (Mak et al., 2023) to warm-start an ADMM algorithm. Both (Kraul et al., 2023) and (Sugishita et al., 2023) use an ML model to predict a initial dual solution in a column-generation algorithm. The most closely-related work is (Qiu et al., 2023), which proposes dual conic proxies for a second-order cone relaxation of the AC Optimal Power Flow problem. In contrast, this paper proposes a general methodology for conic optimization problems that subsumes the approach of (Qiu et al., 2023).

1.2. Contributions and outline

The paper's core contribution is the Dual Lagrangian Learning methodology for learning valid dual bounds for parametric conic optimization problems. In doing so, the paper makes the following contributions.

- The paper presents differentiable conic projection layers. While projecting on a cone is a fundamental operation in many optimization algorithms, its use in a ML context is new;
- The paper proposes a systematic dual completion procedure for recovering dual-feasible solutions, which yield valid Lagrangian dual bounds; In particular, the paper provides a blueprint for building dual completion procedures in non-trivial cases;
- The paper proposes a self-supervised algorithm for dual conic optimization proxies, which emulates the steps of a Lagrangian maximization algorithm;
- The paper conducts numerical experiments on linear and nonlinear conic optimization problems. The results demonstrate the effectiveness of the proposed approach, and motivate the exploitation of problem structure to build a dual completion procedure.

The rest of the paper is organized as follows. Section 2 introduces notations and relevant background material. Section 3 presents the DLL methodology. Section 4 further generalizes DLL, and discusses the advantages of working with conic formulations. Section 5 reports numerical results, and Section 6 concludes the paper.

2. Background

This section introduces relevant notations and standard results on conic optimization and duality, which lay the basis for the proposed learning methodology. The reader is referred to (Ben-Tal & Nemirovski, 2001) for a thorough overview of conic optimization.

2.1. Notations

Unless specified otherwise, the Euclidean norm of a vector $x \in \mathbb{R}^n$ is denoted by $\|x\| = \sqrt{x^\top x}$. The positive and negative part of $x \in \mathbb{R}$ are denoted by $x^+ = \max(0, x)$ and $x^- = \max(0, -x)$. The identity matrix of order n is denoted by I_n , and \mathbf{e} denotes the vector of all ones.

Given a set $\mathcal{X} \subseteq \mathbb{R}^n$, the *interior* and *closure* of \mathcal{X} are denoted by $\text{int } \mathcal{X}$ and by $\text{cl } \mathcal{X}$, respectively. The Euclidean projection onto convex set \mathcal{C} is denoted by $\Pi_{\mathcal{C}}$, where

$$\Pi_{\mathcal{C}}(\bar{x}) = \arg \min_{x \in \mathcal{C}} \|x - \bar{x}\|. \quad (1)$$

The set $\mathcal{K} \subseteq \mathbb{R}^n$ is a *cone* if $x \in \mathcal{K}, \lambda \geq 0 \Rightarrow \lambda x \in \mathcal{K}$, and it is *pointed* if $\mathcal{K} \cap (-\mathcal{K}) = \{0\}$. All cones considered in the paper are *proper* cones, i.e., closed, convex, pointed cones with non-empty interior. The *dual cone* of \mathcal{K} is

$$\mathcal{K}^* = \{y \in \mathbb{R}^n : y^\top x \geq 0, \forall x \in \mathcal{K}\}, \quad (2)$$

and \mathcal{K} is self-dual if $\mathcal{K} = \mathcal{K}^*$. The dual cone of a cartesian product of cones is the cartesian product of the dual cones, i.e., $(\mathcal{K}_1 \times \mathcal{K}_2)^* = \mathcal{K}_1^* \times \mathcal{K}_2^*$.

Given a proper cone $\mathcal{K} \subseteq \mathbb{R}^n$, the *conic inequalities* $\succeq_{\mathcal{K}}$ and $\succ_{\mathcal{K}}$ are defined as

$$\forall (x, y) \in \mathbb{R}^n \times \mathbb{R}^n, x \succeq_{\mathcal{K}} y \Leftrightarrow x - y \in \mathcal{K}, \quad (3a)$$

$$\forall (x, y) \in \mathbb{R}^n \times \mathbb{R}^n, x \succ_{\mathcal{K}} y \Leftrightarrow x - y \in \text{int } \mathcal{K}. \quad (3b)$$

Note that $\succeq_{\mathcal{K}}$ and $\succ_{\mathcal{K}}$ induce a partial and strict partial ordering on \mathbb{R}^n (Ben-Tal & Nemirovski, 2001).

2.2. Standard cones

Most convex optimization problems can be represented using only a small number of cones (Lubin et al., 2016). Standard cones, and their dual cones, are presented next. They are supported by off-the-shelf solvers such as Mosek, ECOS, SCS. The reader is referred to (Coey et al., 2022) for a more exhaustive list of non-standard cones.

Non-negative orthant The non-negative orthant is the self-dual, uni-dimensional cone $\mathbb{R}_+ = \{x \in \mathbb{R} : x \geq 0\}$. It forms the basis of linear programming (Ben-Tal & Nemirovski, 2001).

Second-order cone The second-order cone, also known as Lorentz cone, in dimension n , is defined as

$$\mathcal{Q}^n = \{x \in \mathbb{R}^n : x_1 \geq \|x_2, \dots, x_n\|\}. \quad (4)$$

It is self-dual, i.e., $\mathcal{Q}^* = \mathcal{Q}$.

Rotated Second-Order cone The n -dimensional rotated second-order cone is given by

$$\mathcal{Q}_r^n = \{x \in \mathbb{R}^n : 2x_1 x_2 \geq \|x_3, \dots, x_n\|^2, x_1, x_2 \geq 0\}. \quad (5)$$

This cone forms the building block of conic formulations of convex quadratically-constrained optimization problems.

Semi-Definite Positive cone The semi-definite positive (SDP) cone of order n is defined as

$$\mathcal{S}_+^n = \{X \in \mathbb{R}^{n \times n} : X = X^\top, \lambda_{\min}(X) \geq 0\}, \quad (6)$$

where $\lambda_{\min}(X)$ denotes the smallest eigenvalue of X . Note that all matrices in \mathcal{S}_+ are symmetric, hence all their eigenvalues are real. \mathcal{S}_+ is self-dual.

Exponential Cone The 3-dimensional exponential cone is a non-symmetric cone defined as

$$\mathcal{E} = \text{cl} \left\{ x \in \mathbb{R}^3 : x_1 \geq x_2 e^{x_3/x_2}, x_2 > 0 \right\}. \quad (7)$$

Its dual cone is defined as

$$\mathcal{E}^* = \text{cl} \left\{ y \in \mathbb{R}^3 : \frac{-y_1}{y_3} \geq e^{\frac{y_2}{y_3}-1}, y_1 > 0, y_3 < 0 \right\}. \quad (8)$$

The exponential cone is useful to model exponential and logarithmic terms, for instance relative entropy terms.

Power Cone Power cones are non-symmetric cones, which allow to express power other than 2. In particular, power cones allow to express p -norms with $p \geq 1$. The paper focuses on the 3-dimensional power cone

$$\mathcal{P}_\alpha = \left\{ x \in \mathbb{R}^3 : x_1^\alpha x_2^{1-\alpha} \geq |x_3|, x_1, x_2 \geq 0 \right\} \quad (9)$$

for $0 < \alpha < 1$, which is sufficient to express more general, high-dimensional power cones. The dual power cone is

$$\mathcal{P}_\alpha^* = \left\{ y \in \mathbb{R}^3 : \left(\frac{y_1}{\alpha}, \frac{y_2}{1-\alpha}, y_3 \right) \in \mathcal{P}_\alpha \right\}. \quad (10)$$

2.3. Conic duality

Consider a conic optimization problem of the form

$$\min_x \quad c^\top x \quad (11a)$$

$$\text{s.t.} \quad Ax \succeq_{\mathcal{K}} b, \quad (11b)$$

$$l \leq x \leq u, \quad (11c)$$

where $c, l, u \in \mathbb{R}^n$, $b \in \mathbb{R}^m$, $A \in \mathbb{R}^{m \times n}$, and \mathcal{K} is a proper cone. The corresponding dual problem reads

$$\max_{y, z^l, z^u} \quad b^\top y + l^\top z^l - u^\top z^u \quad (12a)$$

$$\text{s.t.} \quad A^\top y + z^l - z^u = c, \quad (12b)$$

$$y \in \mathcal{K}^*, z^l, z^u \geq 0. \quad (12c)$$

The paper makes the following assumptions.

Assumption 2.1. All variable bounds are finite, non-trivial and consistent, i.e., $-\infty < l_j < u_j < +\infty, \forall j \in \{1, \dots, n\}$.

The condition $l_j < u_j$ in Assumption 2.1 is easily enforced in a pre-processing step. Indeed, if $l_j > u_j$ for $j \in \{1, \dots, n\}$, then Problem (11) is trivially infeasible. Likewise, if $l_j = u_j$ for some $j \in \{1, \dots, n\}$, then variable x_j is fixed and can be removed from the problem. Finally, in most –if not all– real-life settings, decision variables are physical quantities (e.g. budgets or production levels) that are naturally bounded. Hence, Assumption 2.1 holds in most practical cases. Section 4.1 extends the DLL methodology to the general case, without explicit variable bounds.

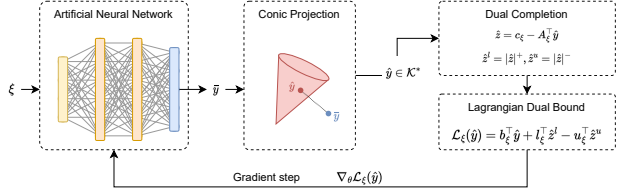


Figure 1. Illustration of the proposed DLL scheme. Given an input parameter ξ , a neural network first predicts $\bar{y} \in \mathbb{R}^n$. Then, a conic projection layer computes a conic-feasible $\hat{y} \in \mathcal{K}^*$. Finally, a dual completion step recovers dual-feasible solution $(\hat{y}, \hat{z}^l, \hat{z}^u)$. The model is trained in a self-supervised fashion by maximizing the Lagrangian dual bound $\mathcal{L}(\hat{y})$.

Assumption 2.2. Slater’s constraint qualification holds for the primal problem, i.e., $\exists x \in [l, u] : Ax \succ_{\mathcal{K}} b$.

Assumption 2.2 holds in most practical cases, and can be enforced via, e.g., soft constraints. It is important to note that the use of soft constraints to ensure feasibility is a common practice in most industry settings.

Assumptions 2.1 and 2.2 ensure that conic strong duality holds (Ben-Tal & Nemirovski, 2001): both primal and dual problems are solvable with identical optimal values.

3. Dual Lagrangian Learning (DLL)

This section presents the *Dual Lagrangian Learning* (DLL) methodology for learning dual bounds for conic optimization problems. Consider a parametric conic optimization problem, with parameters $\xi \in \Xi$, of the form

$$P_\xi \quad \min_x \quad c_\xi^\top x \quad (13a)$$

$$\text{s.t.} \quad A_\xi x \succeq_{\mathcal{K}} b_\xi, \quad (13b)$$

$$l_\xi \leq x \leq u_\xi, \quad (13c)$$

whose parametric dual problem reads

$$D_\xi \quad \max_{y, z^l, z^u} \quad b_\xi^\top y - l_\xi^\top z^l - u_\xi^\top z^u \quad (14a)$$

$$\text{s.t.} \quad A_\xi^\top y + z^l - z^u = c_\xi, \quad (14b)$$

$$y \in \mathcal{K}^*, z^l, z^u \geq 0. \quad (14c)$$

Recall that Slater’s condition and, in turn, strong duality, are assumed to hold, i.e., $\forall \xi \in \Xi$, P_ξ and D_ξ are solvable and have same (finite) objective value.

Figure 1 illustrates the proposed Dual Lagrangian Learning (DLL) methodology. DLL combines the representation power of artificial neural networks (or, more generally, any differentiable program), with conic duality theory, to provide valid Lagrangian dual bounds for general conic optimization problems. To that end, DLL exploits three fundamental building blocks:

1. A (sub)differentiable conic projection layer that, given $\bar{y} \in \mathbb{R}^n$, outputs dual conic-feasible $\hat{y} \in \mathcal{K}^*$;
2. A dual completion procedure that computes a valid Lagrangian dual bound $\mathcal{L}(\hat{y})$ and, as a by-product, provides a dual-feasible solution $(\hat{y}, \hat{z}^l, \hat{z}^u)$;
3. A self-supervised learning algorithm that emulates the steps of a dual Lagrangian maximization algorithm.

Each of these building blocks is presented next.

3.1. Dual Conic Projection

The first building block of DLL are conic projection layers, which project an input $\bar{y} \in \mathbb{R}^n$ onto $\hat{y} \in \mathcal{K}^*$. It is important to note that the correctness of DLL only requires a valid projection onto \mathcal{K}^* , which need not be the Euclidean projection $\Pi_{\mathcal{K}^*}$; indeed, the latter may be computationally expensive and cumbersome to differentiate. The paper presents valid projection operators for each standard cone and its dual; these projections are simple to implement, computationally fast, and differentiable almost everywhere. The reader is referred to (Parikh et al., 2014), Sec. 6.3, for an overview of Euclidean projections onto standard cones.

Recall that $\mathbb{R}_+, \mathcal{Q}, \mathcal{Q}_r, \mathcal{S}_+$ are self-dual cones, for which projecting onto the dual cone \mathcal{K}^* is equivalent to projecting onto the primal cone \mathcal{K} . For the non self-dual cones \mathcal{E} and \mathcal{P} , the paper provides, for completeness, projection operators for both the primal and dual cones.

Non-negative orthant The Euclidean projection on \mathbb{R}_+ is trivial using the well-known ReLU function:

$$\hat{y} = \Pi_{\mathbb{R}_+}(\bar{y}) = \max(0, \bar{y}) = \text{ReLU}(\bar{y}). \quad (15)$$

Second-order cone The Euclidean projection on \mathcal{Q}^n is

$$\Pi_{\mathcal{Q}^n}(\bar{y}) = \begin{cases} \bar{y} & \text{if } \bar{y} \in \mathcal{Q}^n \\ 0 & \text{if } \bar{y} \in -\mathcal{Q}^n \\ \frac{\bar{y}_1 + \delta}{2\delta}(\delta, \bar{y}_{2:n}) & \text{otherwise} \end{cases} \quad (16)$$

where $\bar{y}_{2:n} = (\bar{y}_2, \dots, \bar{y}_n)$ and $\delta = \|\bar{y}_{2:n}\|$. The main drawback of $\Pi_{\mathcal{Q}^n}$ is that it is identically zero on $-\mathcal{Q}^n$, which is not desirable when training artificial neural networks as it may cause gradient vanishing. The simpler formula

$$\hat{y} = (\hat{y}_1, \bar{y}_2, \dots, \bar{y}_n), \quad \hat{y}_1 = \max(\bar{y}_1, \|\bar{y}_2, \dots, \bar{y}_n\|), \quad (17)$$

can be used instead: it is efficient and not identically zero on $-\mathcal{Q}^n$. The same approach is used to project onto \mathcal{Q}_r .

SDP cone The Euclidean projection onto \mathcal{S}_+^n of $\bar{Y} \in \mathcal{S}^n$ with eigenvalue decomposition $\bar{Y} = \sum_i \lambda_i v_i v_i^\top$ is

$$\Pi_{\mathcal{S}_+^n}(\bar{Y}) = \sum_i \max(0, \lambda_i) v_i v_i^\top. \quad (18)$$

To avoid the cost of a full eigenvalue decomposition, which has complexity $\mathcal{O}(n^3)$, a simpler projection

$$\hat{Y} = \bar{Y} + \lambda_{\min}(\bar{Y}) I_n, \quad (19)$$

can be used instead: it only requires a smallest eigenvalue computation, and only modifies the diagonal of \bar{Y} .

Exponential Cone To the best of the authors' knowledge, there is no closed-form, analytical formula for evaluating $\Pi_{\mathcal{E}}$ nor $\Pi_{\mathcal{E}^*}$, which instead require a root-finding operation, see, e.g., (Parikh et al., 2014) and (Friberg, 2023). To project \bar{x} onto \mathcal{E} , a possible approach is to use

$$\hat{x}_1 = \bar{x}_1, \quad \hat{x}_2 = \bar{x}_2, \quad \hat{x}_3 = \min\left(\bar{x}_3, \bar{x}_2 \log \frac{\bar{x}_1}{\bar{x}_2}\right) \quad (20)$$

for $\bar{x}_1, \bar{x}_2 > 0$. It reduces to $\hat{x}_3 = \min(\bar{x}_3, 0)$ as $\bar{x}_2 \rightarrow 0$. This approach does not require any root-finding, and is therefore more amenable to automatic differentiation. The validity of Eq. (20) is immediate from the representation

$$\mathcal{E} = \text{cl}\{x \in \mathbb{R}^3 : \frac{x_3}{x_2} \leq \log \frac{x_1}{x_2}, x_1, x_2 > 0\}, \quad (21)$$

Similarly, to project on \mathcal{E}^* , a possible approach is to use

$$\hat{y}_1 = \bar{y}_1, \quad \hat{y}_2 = \max\left(\bar{y}_2, \bar{y}_3 + \bar{y}_3 \ln \frac{\bar{y}_1}{-\bar{y}_3}\right), \quad \hat{y}_3 = \bar{y}_3, \quad (22)$$

for $\bar{y}_1 > 0$ and $\bar{y}_3 < 0$.

Power Cone Let $0 < \alpha < 1$. The Euclidean projection onto the power cone \mathcal{P}_α is described in (Hien, 2015). Similar to the exponential cone, it requires a root-finding operation. Thus, the paper proposes simpler, non-Euclidean projections for \mathcal{P}_α and \mathcal{P}_α^* . The primal projection reads

$$\hat{x}_1 = \max\left(\bar{x}_1, \bar{x}_2^{\frac{\alpha-1}{\alpha}} |\bar{x}_3|^{\frac{1}{\alpha}}\right), \quad \hat{x}_2 = \bar{x}_2, \quad \hat{x}_3 = \bar{x}_3. \quad (23)$$

A similar approach is done to recover $y \in \mathcal{P}_\alpha^*$ after scaling the first two coordinates of y . This technique can be extended to the more general power cones.

3.2. Lagrangian Dual Bounds

The second building block of DLL is the derivation of valid dual bounds. DLL uses the Lagrangian dual bound

$$\mathcal{L}_\xi(\hat{y}) = \min_{l_\xi \leq x \leq u_\xi} c_\xi^\top x + (b_\xi - A_\xi x)^\top \hat{y}, \quad (24)$$

for $\hat{y} \in \mathcal{K}^*$. Noting that Eq. (24) minimizes a linear function over a bounded box-shaped domain, it follows that

$$\mathcal{L}_\xi(\hat{y}) = b_\xi^\top \hat{y} + l_\xi^\top |c_\xi - A_\xi^\top \hat{y}|^+ - u_\xi^\top |c_\xi - A_\xi^\top \hat{y}|^-. \quad (25)$$

The above derivation of $\mathcal{L}_\xi(\hat{y})$ is equivalent to the following dual completion procedure. Given $\hat{y} \in \mathcal{K}^*$, define

$\hat{z} = c_\xi - A_\xi^\top \hat{y}$ and let $\hat{z}^l = |\hat{z}|^+$, $\hat{z}^u = |\hat{z}|^-$. By construction $(\hat{y}, \hat{z}^l, \hat{z}^u)$ is a dual feasible solution for the dual problem (14). Furthermore, it is immediate to verify that (\hat{z}^l, \hat{z}^u) is an optimal solution of

$$\max_{z^l, z^u} l_\xi^\top z^l - u_\xi^\top z^u + b_\xi^\top \hat{y} \quad (26a)$$

$$s.t. \quad z^l - z^u = c_\xi - A_\xi^\top \hat{y}, \quad (26b)$$

$$z^l, z^u \geq 0, \quad (26c)$$

whose optimal value is exactly the Lagrangian bound $\mathcal{L}_\xi(\hat{y})$. This dual perspective shows that $\mathcal{L}_\xi(\hat{y})$ is a valid dual bound (by weak duality), and that it is the strongest possible dual bound given $\hat{y} \in \mathcal{K}^*$. It also is important to note that (\hat{z}^l, \hat{z}^u) are obtained “for free” when computing $\mathcal{L}_\xi(\hat{y})$ using Eq. (25), thus providing a systematic dual completion procedure with dual feasibility guarantees.

3.3. Self-Supervised Dual Lagrangian Training

The third building block of DLL is a self-supervised training algorithm based on the dual Lagrangian problem. For fixed parameter ξ , the dual Lagrangian problem reads

$$\max_{\hat{y}} \quad \{\mathcal{L}_\xi(\hat{y}) : \hat{y} \in \mathcal{K}^*\}, \quad (27)$$

i.e., it seeks a dual vector $\hat{y} \in \mathcal{K}^*$ that maximizes the Lagrangian bound $\mathcal{L}_\xi(\hat{y})$. Note that (27) is equivalent to the dual problem (14), whose optimal value is equal to the optimal value of (13) when strong duality holds. The Lagrangian dual problem (27) provides the basis for the proposed self-supervised algorithm outlined below. *To the best of the authors’ knowledge, this paper is the first to propose a principled self-supervised framework with dual guarantees for general conic optimization problems.*

Let \mathcal{M}_θ be a differentiable program, parametrized by θ , which takes ξ as input and outputs $\hat{y} \in \mathcal{K}^*$. Recall that the output condition $\hat{y} \in \mathcal{K}^*$ can be enforced via the dual conic projection presented in Section 3.1. Given a dataset $(\xi^{(1)}, \dots, \xi^{(N)})$, the self-supervised training problem is formulated as

$$\max_{\theta} \quad \frac{1}{N} \sum_i \mathcal{L}_{\xi^{(i)}} \left(\mathcal{M}_\theta(\xi^{(i)}) \right), \quad (28)$$

i.e., it finds the value of θ that maximizes the average Lagrangian dual bound over the dataset.

The self-supervised training problem (28) can be solved by, e.g., a stochastic (sub)gradient algorithm, using automatic differentiation to compute gradient information. Note that, instead of updating \hat{y} directly using a (sub)gradient $\partial_y \mathcal{L}_\xi(y)$, the training procedure computes a subgradient $\frac{1}{N} \sum_i \partial_{\theta} \mathcal{L}_{\xi^{(i)}}(\hat{y}^{(i)})$ to update θ and then obtains the new prediction $\hat{y}^{(i)}$ through \mathcal{M}_θ .

4. Extensions

4.1. Problems without Variable Bounds

Although most real-life problems are typically bounded, not all primal variables may have explicit finite lower and upper bounds, thus invalidating Assumption 2.1. This section presents two strategies for dealing with this case; see Section 5.2 for a numerical comparison.

Consider a conic optimization problem of the form

$$\min_x \quad c^\top x \quad (29a)$$

$$s.t. \quad Ax \succeq_{\mathcal{K}} b, \quad (29b)$$

$$Hx \succeq_{\mathcal{C}} h, \quad (29c)$$

where \mathcal{K}, \mathcal{C} are proper cones. Note that (29) does not include explicit bounds on primal variables. The dual problem is

$$\max_{y, \lambda} \quad b^\top y + h^\top \lambda \quad (30a)$$

$$s.t. \quad A^\top y + H^\top \lambda = c, \quad (30b)$$

$$y \in \mathcal{K}^*, \lambda \in \mathcal{C}^*. \quad (30c)$$

The first, most straightforward, strategy, is to compute lower and upper bounds for each variable. Valid bounds can be obtained from domain knowledge, or by solving

$$l_j = \min_x \{x_j : (29b), (29c)\}, \quad (31a)$$

$$u_j = \max_x \{x_j : (29b), (29c)\}. \quad (31b)$$

Naturally, solving all $2n$ problems in (31) may be computationally cumbersome, and may fail to yield finite bounds. Note however that valid bounds can be obtained from any valid relaxation of (31), which may be more tractable. Furthermore, one may include a so-called objective cut of the form $c^\top x \leq M$ to (31), where M is a valid upper bound on the optimal value of (29); this approach may provide tighter bounds, and does not remove any optimal solution.

Once valid, finite bounds l, u are identified, one can apply DLL out of the box. Namely, given a dual prediction $y \in \mathcal{K}^*, \lambda \in \mathcal{C}^*$, the Lagrangian bound is

$$\mathcal{L}(y, \lambda) = \min_{l \leq x \leq u} c^\top x + (b - Ax)^\top y + (h - Hx)^\top \lambda. \quad (32)$$

Note that the Lagrangian bound $\mathcal{L}(y, \lambda)$ depends on the value of l, u . Therefore, weaker variable bounds yield weaker dual bounds.

The second strategy leverages a more general result (Theorem 4.1) for computing Lagrangian dual bounds and, equivalently, recovering dual-feasible solutions.

Theorem 4.1. *Assume that $\forall y \in \mathcal{K}^*$, the problem*

$$\tilde{\mathcal{L}}(y) = \min_x \quad c^\top x + (b - Ax)^\top y \quad (33a)$$

$$s.t. \quad Hx \succeq_{\mathcal{C}} h \quad (33b)$$

is bounded and satisfies Slater’s condition. Then $\forall y \in \mathcal{K}^*$, $\tilde{\mathcal{L}}(y)$ is finite, and $\exists \tilde{\lambda} \in \mathcal{C}^*$ such that $(y, \tilde{\lambda})$ is feasible for the dual problem (30) with dual objective value $\tilde{\mathcal{L}}(y)$.

Proof. Let $y \in \mathcal{K}^*$. The dual problem of (33) reads

$$\max_{\lambda} b^\top y + h^\top \lambda \quad (34a)$$

$$s.t. \quad H^\top \lambda = c - A^\top y, \quad (34b)$$

$$\lambda \in \mathcal{C}^*. \quad (34c)$$

Slater’s condition ensures that conic strong duality holds (Ben-Tal & Nemirovski, 2001). Therefore, (33) and (34) are solvable with finite objective value, hence, $\tilde{\mathcal{L}}(y)$ is finite. Next, let $\tilde{\lambda}$ be an optimal solution of (34). By construction, $\tilde{\lambda} \in \mathcal{C}^*$, and $(y, \tilde{\lambda})$ is feasible for Problem (30) with dual objective value $b^\top y + h^\top \tilde{\lambda} = \tilde{\mathcal{L}}(y)$. \square

Unlike the results of Section 3.2, Theorem 4.1 only provides an existence result: there is no general, closed-form formulae for constructing λ nor computing the Lagrangian bound $\mathcal{L}(y)$. Nevertheless, when additional problem structure is known, Theorem 4.1 provides a blueprint for building a dual completion procedure and applying DLL. First, identify a subset of constraints that, akin to constraints (29c), are sufficient to ensure boundedness of the primal problem. Second, build a dual completion procedure that recovers λ given $y \in \mathcal{K}^*$. This is arguably the most challenging step, and requires domain knowledge unless one uses an implicit layer to solve (34). Third, construct a differentiable program \mathcal{M}_θ that produces $\hat{y} \in \mathcal{K}^*$. Fourth, train \mathcal{M}_θ using the dual completion step and the self-supervised learning framework presented in Section 3.3.

4.2. Nonlinear Convex Optimization

Convex optimization problems are often formulated in a nonlinear, “function-based” form. While the paper’s DLL approach extends to this setting, this section outlines the advantages of conic-based formulations. Consider a convex optimization problem of the form

$$\min_x f(x) \quad (35a)$$

$$s.t. \quad g_i(x) \leq 0, \quad \forall i = 1, \dots, m \quad (35b)$$

$$l \leq x \leq u, \quad (35c)$$

where f, g are convex functions, $-\infty < l < u < +\infty$ and assume Slater’s constraint qualification holds. Given $y \geq 0$, the Lagrangian dual bound is then

$$\mathcal{L}(y) = \min_{l \leq x \leq u} f(x) + \sum_i y_i g_i(x), \quad (36)$$

which is the convex optimization counterpart of Eq. (24). Therefore, comparing Eq. (36) with Eq. (24) yields valuable insights into the advantages of a conic formulation.

On the one hand, to obtain a valid Lagrangian dual bound, one must enforce $y \in \mathcal{K}^*$ in the conic setting, which is more restrictive than $y \geq 0$ in the convex setting. Nevertheless, the conic projection layers presented in Section 3.1 provide computationally efficient tools to produce conic-feasible solutions, i.e., $y \in \mathcal{K}^*$.

On the other hand, the conic setting allows for a straightforward evaluation of the Lagrangian dual bound, via Eq. (25), which has the added advantage of being directly amenable to automatic differentiation. In contrast, there is no closed-form, analytical solution to (36) in general. Thus, DLL would require the use of a numerical method, both for training and inference. Moreover, computing (sub)gradients $\partial_y \mathcal{L}$ would require either using costly implicit layers (Agrawal et al., 2019), or manually providing gradient information to the AD backend. Hence, from a computational standpoint, the conic approach is simpler to implement, less error-prone, less application-specific and, in general, more efficient.

In summary, the conic form yields substantial advantages in terms of simplicity and generality, compared to nonlinear programming-based formulations. Note also that tools such as Disciplined Convex Programming (Grant et al., 2006) can automatically reformulate convex programs into their conic forms.

5. Numerical experiments

This section presents numerical experiments on two classes of problems: the linear relaxation of the multi-dimensional knapsack problem, and a nonlinear production and inventory planning problem. The former satisfies Assumptions 2.1 and 2.2. The latter only satisfies Assumption 2.2, and therefore illustrates the methodology presented in Section 4.1. Experiment settings are reported in Appendix A.

5.1. Multi-dimensional knapsack

5.1.1. PROBLEM FORMULATION

Consider multi-dimensional knapsack problems (Freville & Plateau, 1994; Freville, 2004), which are of the form

$$\min_x -p^\top x \quad (37a)$$

$$s.t. \quad Wx \leq b, \quad (37b)$$

$$x_i \in \{0, 1\}, \quad \forall j = 1, \dots, n \quad (37c)$$

where $p \in \mathbb{R}^n$ denotes the value of each item, $W \in \mathbb{R}^{m \times n}$ is a weight matrix, and $b \in \mathbb{R}^m$ denotes the capacity of each knapsack. The continuous relaxation is obtained by relaxing the binary constraints (37c) into $0 \leq x_j \leq 1, \forall j$. The dual

Table 1. Optimality gaps achieved by DLL on multi-dimensional knapsack instances.

m	n	Test gap (%)			
		avg	std	min	max
5	100	0.37	0.20	0.01	1.36
	200	0.18	0.11	0.01	0.84
	500	0.08	0.05	0.00	0.35
10	100	0.68	0.25	0.10	1.86
	200	0.35	0.14	0.06	1.03
	500	0.14	0.06	0.02	0.48
30	100	1.93	0.37	0.88	3.30
	200	0.96	0.20	0.40	1.83
	500	0.38	0.09	0.14	0.75

All gaps are measured w.r.t Gurobi's LP relaxation

problem reads

$$\max_{y, z^l, z^u} b^\top y - f^\top z^u \quad (38a)$$

$$s.t. \quad W^\top y + z^l - z^u = -p \quad (38b)$$

$$y \leq 0, z^l, z^u \geq 0, \quad (38c)$$

where $y \in \mathbb{R}^m$ and $z^l, z^u \in \mathbb{R}^n$. Thus, the Lagrangian is

$$\mathcal{L}(y) = b^\top y - \mathbf{e}^\top | -p - W^\top y |^- \quad (39)$$

5.1.2. RESULTS

Numerical results are presented in Table 1 which reports, for each combination of number of resources (m) and items (n): the average (avg) optimality gap, the standard deviation (std) of optimality gaps, and the minimum (min) and maximum (max) optimality gap achieved on the test set. The optimality gap for instance i is measured as

$$\text{gap}_i = \frac{\mathcal{L}(\hat{y}_i) - \mathcal{L}(y_i^*)}{\mathcal{L}(y_i^*)}, \quad (40)$$

where \hat{y}_i and y_i^* denote the predicted dual variables, obtained from the trained FCNN, and the optimal dual solution, obtained with Gurobi.

The results of Table 1 motivate the following comments. First, average optimality gaps range from 0.08% when $(m, n) = (5, 500)$, to 1.93% when $(m, n) = (30, 100)$. Second, an interesting trend can be identified: larger values of m yield higher optimality gaps, while higher values of n yield smaller optimality gaps. This effect may be explained by the fact that increasing m increases the output dimension of the FCNN: larger output dimensions are typically harder to predict. In addition, a larger n likely provides a smoothing effect on the dual, whose solution becomes easier to

predict. The reader is referred to (Freville, 2004) for probabilistic results on properties of multi-knapsack problems. A similar behavior is observed for minimum and maximum optimality gaps.

5.2. Production and Inventory Planning

5.2.1. PROBLEM FORMULATION

Consider the resource-constrained production and inventory planning problem (Ziegler, 1982; MOSEK Aps, 2023b)

$$\min_{x, t} d^\top x + f^\top t \quad (41a)$$

$$s.t. \quad r^\top x \leq b, \quad (41b)$$

$$(x_j, t_j, \sqrt{2}) \in \mathcal{Q}_r^3, \quad \forall j = 1, \dots, n. \quad (41c)$$

where n is the number of items to be produced, $x \in \mathbb{R}^n$, $b \in \mathbb{R}$ denotes the available resource amount, and $r_j > 0$ denotes the resource consumption rate of item j . The objective function captures production and inventory costs. Namely, $d_j = \frac{1}{2} c_j^p c_j^r$ and $f_j = c_j^o D_j$, where $c_j^p, c_j^r, c_j^o > 0$ and $D_j > 0$ denote per-unit holding cost, rate of holding cost, ordering cost, and total demand for item j , respectively.

Since primal variables do not have explicit bounds, (41) falls under the setting of Section 4.1. In particular, the feasible domain of t is unbounded, which is common when using an epigraph reformulation of a convex objective. Nevertheless, the following bounds hold for all optimal solutions:

$$0 \leq x_j \leq br_j^{-1}, \quad 0 \leq t_j \leq Mf_j^{-1}, \quad (42)$$

where $M = d^\top \bar{x} + f^\top \bar{x}^{-1}$ and $\bar{x}_j = n^{-1} r_j^{-1} b, \forall j$. This yields the bounded formulation

$$\min_{x, t} \{d^\top x + f^\top t : (41b), (41c), (42)\}. \quad (43)$$

5.2.2. DUAL COMPLETION

The dual problem is stated for the bounded form (43):

$$\max_{y, \pi, \tau, \sigma, z} by - \sqrt{2} \mathbf{e}^\top \sigma_j - u_x^\top z_x^u - u_t^\top z_t^u \quad (44a)$$

$$s.t. \quad ry + \pi + z_x^l - z_x^u = d, \quad (44b)$$

$$\tau + z_t^l - z_t^u = f, \quad (44c)$$

$$y \leq 0, \quad (44d)$$

$$(\pi_j, \tau_j, \sigma_j) \in \mathcal{Q}_r^3, \quad \forall j = 1, \dots, n, \quad (44e)$$

$$z_x^l, z_x^u, z_t^l, z_t^u \geq 0, \quad (44f)$$

where z_x^l, z_x^u and z_t^l, z_t^u are the dual variables associated with lower/upper bounds on x and t , respectively. The corresponding Lagrangian is

$$\hat{\mathcal{L}}(\hat{y}, \hat{\pi}, \hat{\tau}, \hat{\sigma}) = b\hat{y} - \sqrt{2} f^\top \hat{\sigma} - u_x^\top |\hat{z}_x|^- - u_t^\top |\hat{z}_t|^-, \quad (45)$$

Table 2. Numerical results on production planning instances.

n	Bounded form (43)			Original form (41)		
	avg.	std	max	avg.	std	max
10	79.95	6.63	93.34	0.19	0.40	9.93
20	84.33	4.94	94.02	0.35	0.66	12.34
50	85.27	4.35	94.28	1.27	2.33	36.96
100	85.58	3.86	93.16	0.74	1.16	13.10
200	86.44	3.77	94.08	0.31	0.46	5.22
500	87.21	3.67	93.96	0.36	0.55	7.48
1000	87.21	3.66	93.95	0.66	1.04	11.60

where $\hat{z}_x = d - r\hat{y} - \hat{\pi}$ and $\hat{z}_t = f - \hat{\tau}$.

Fixing $z_x^l, z_x^u, z_t^l, z_t^u = 0$ in (46) yields the dual of (41):

$$\max_{y, \pi, \tau, \sigma} by - \sqrt{2}\mathbf{e}^\top \sigma \quad (46a)$$

$$s.t. \quad ry + \pi = d, \quad (46b)$$

$$\tau = f, \quad (46c)$$

$$y \leq 0, \quad (46d)$$

$$(\pi_j, \tau_j, \sigma_j) \in \mathcal{Q}_r^3, \quad \forall j = 1 \dots n. \quad (46e)$$

The dual problem (46) suggests the following dual completion procedure. Assume $\tilde{y} \leq 0$ is given. Constraints (46c) and (46b) yield $\tilde{\tau} = f$ and $\tilde{\pi} = d - r\tilde{y}$; note that $\tilde{\pi}, \tilde{\tau} > 0$, because $d, f, r > 0$ and $\tilde{y} \leq 0$. Next, noting that σ has negative objective coefficient and appears only in constraint (46e), it follows that $\tilde{\sigma}_j = -\sqrt{2}\tilde{\pi}_j\tilde{\tau}_j$. The resulting Lagrangian is

$$\tilde{\mathcal{L}}(\tilde{y}) = b\tilde{y} + \sum_j 2\sqrt{f_j(d_j - r_j\tilde{y})}. \quad (47)$$

5.2.3. RESULTS

Table 2 reports the test performance of each model, for various values of n . Namely, the table reports, for each approach (bounded vs original formulation), the average (avg), standard deviation (std) and maximum (max) optimality gap across the test set. Recall that optimality gaps measure the quality of the learned Lagrangian bound, namely $\tilde{\mathcal{L}}(\hat{y})$ for the bounded formulation and $\tilde{\mathcal{L}}(\tilde{y})$ for the original formulation, against $\tilde{\mathcal{L}}(y^*)$, where y^* is the optimal solution reported by Mosek; see Eq. (40).

The results of Table 2 shows that working with the original formulation yields significantly better results than using artificial variable bounds. Namely, while the average gap achieved by the bounded formulation ranges between 80% and 87.2%, the original form with dual completion achieves average optimality gaps as low as 0.19% ($n=10$) and almost always below 1%. This represents an improvement of more than two orders of magnitude compared to the bounded

formulation. Similarly, significant improvements in maximum optimality gaps are observed when using the original formulation.

The above results can be explained by several factors. First, the bounded formulation significantly increases the dimension of the dual solution to predict: $3n + 1$, compared to 1 when working with the original formulation. This naturally complicates the learning task. Second, the introduction of variable bounds create additional terms $-u_x^\top z_x^u - u_t^\top z_t^u$ in the Lagrangian function (45). This, in turn, likely makes the gradient $\nabla \tilde{\mathcal{L}}$ less informative, further slowing training. Third, the bounded formulation does not exploit the rich structure of the dual problem (46); instead, the ML model must learn such constraints using only the loss information. The results of Table 2 suggest that the model is not able to learn these simple constraints.

These results demonstrate the benefits of exploiting domain knowledge when possible and, in particular, of using dual constraints to simplify the dual learning task. Doing so allows for smaller models that are more memory-efficient and easier to train, and results in more informative gradients.

6. Conclusion

The paper has proposed Dual Lagrangian Learning, a principled methodology for learning valid dual bounds for parametric conic optimization problems. To that end, the paper has presented conic projection layers, a systematic dual completion procedure, and a self-supervised learning algorithm. The effectiveness of DLL has been demonstrated on numerical experiments consider linear and nonlinear conic problems. In particular, results have shown that exploiting problem structure, when possible, yields simpler models and improved performance.

DLL opens the door to multiple avenues for future research, at the intersection of ML and optimization. The availability of high-quality dual-feasible solutions naturally calls for the integration of DLL in existing optimization algorithms, either as a warm-start, or to obtain good dual bounds fast. Multiple optimization algorithms have been proposed to optimize Lagrangian functions, which may yield more efficient training algorithms in DLL. Finally, given the importance of conic optimization in numerous real-life applications, DLL can provide a useful complement to existing primal proxies.

Acknowledgments

This work was partially funded by NSF grant 2112533 and ARPA-E PERFORM award AR0001136.

References

Agrawal, A., Amos, B., Barratt, S., Boyd, S., Diamond, S., and Kolter, J. Z. Differentiable convex optimization layers. In Wallach, H., Larochelle, H., Beygelzimer, A., d’Alché-Buc, F., Fox, E., and Garnett, R. (eds.), *Advances in Neural Information Processing Systems*, volume 32. Curran Associates, Inc., 2019. URL https://proceedings.neurips.cc/paper_files/paper/2019/file/9ce3c52fc54362e22053399d3181c638-Paper.pdf.

Bello, I., Pham, H., Le, Q. V., Norouzi, M., and Bengio, S. Neural combinatorial optimization with reinforcement learning. *arXiv preprint arXiv:1611.09940*, 2016.

Ben-Tal, A. and Nemirovski, A. *Lectures on modern convex optimization: analysis, algorithms, and engineering applications*. SIAM, 2001.

Bengio, Y., Lodi, A., and Prouvost, A. Machine learning for combinatorial optimization: A methodological tour d’horizon. *European Journal of Operational Research*, 290(2):405–421, 2021. ISSN 0377-2217. doi: <https://doi.org/10.1016/j.ejor.2020.07.063>.

Chen, W., Tanneau, M., and Hentenryck, P. V. End-to-End Feasible Optimization Proxies for Large-Scale Economic Dispatch. *IEEE Transactions on Power Systems*, pp. 1–12, 2023. doi: [10.1109/TPWRS.2023.3317352](https://doi.org/10.1109/TPWRS.2023.3317352).

Coey, C., Kapelevich, L., and Vielma, J. P. Solving natural conic formulations with hypatia.jl. *INFORMS Journal on Computing*, 34(5):2686–2699, 2022. doi: [10.1287/ijoc.2022.1202](https://doi.org/10.1287/ijoc.2022.1202).

Donti, P. L., Rolnick, D., and Kolter, J. Z. DC3: A learning method for optimization with hard constraints. In *9th International Conference on Learning Representations, ICLR 2021, Virtual Event, Austria, May 3-7, 2021*, 2021. URL <https://iclr.cc/virtual/2021/poster/2868>.

Fiorotto, F., Mak, T. W., and Van Hentenryck, P. Predicting AC Optimal Power Flows: Combining deep learning and lagrangian dual methods. In *Proceedings of the AAAI conference on artificial intelligence*, volume 34, pp. 630–637, 2020. URL <https://doi.org/10.1609/aaai.v34i01.5403>.

Freville, A. The multidimensional 0–1 knapsack problem: An overview. *European Journal of Operational Research*, 155(1):1–21, 2004. ISSN 0377-2217. doi: [10.1016/S0377-2217\(03\)00274-1](https://doi.org/10.1016/S0377-2217(03)00274-1).

Freville, A. and Plateau, G. An efficient preprocessing procedure for the multidimensional 0–1 knapsack problem. *Discrete Applied Mathematics*, 49(1):189–212, 1994. ISSN 0166-218X. doi: [10.1016/0166-218X\(94\)90209-7](https://doi.org/10.1016/0166-218X(94)90209-7). Special Volume Viewpoints on Optimization.

Friberg, H. A. Projection onto the exponential cone: a univariate root-finding problem. *Optimization Methods and Software*, 38(3):457–473, 2023. doi: [10.1080/10556788.2021.2022147](https://doi.org/10.1080/10556788.2021.2022147).

Grant, M., Boyd, S., and Ye, Y. Disciplined convex programming. *Global optimization: From theory to implementation*, pp. 155–210, 2006.

Gurobi Optimization, L. Gurobi optimizer reference manual, 2018. URL <https://www.gurobi.com>.

Hien, L. T. K. Differential properties of euclidean projection onto power cone. *Mathematical Methods of Operations Research*, 82:265–284, 2015.

Innes, M. Don’t unroll adjoint: Differentiating ssa-form programs. *CoRR*, abs/1810.07951, 2018. URL <https://arxiv.org/abs/1810.07951>.

Innes, M., Saba, E., Fischer, K., Gandhi, D., Rudilosso, M. C., Joy, N. M., Karmali, T., Pal, A., and Shah, V. Fashionable modelling with flux. *CoRR*, abs/1811.01457, 2018. URL <https://arxiv.org/abs/1811.01457>.

Khalil, E., Dai, H., Zhang, Y., Dilkina, B., and Song, L. Learning combinatorial optimization algorithms over graphs. *Advances in neural information processing systems*, 30, 2017.

Kotary, J., Fiorotto, F., Van Hentenryck, P., and Wilder, B. End-to-end constrained optimization learning: A survey. In Zhou, Z.-H. (ed.), *Proceedings of the Thirtieth International Joint Conference on Artificial Intelligence, IJCAI-21*, pp. 4475–4482. International Joint Conferences on Artificial Intelligence Organization, 8 2021. doi: [10.24963/ijcai.2021/610](https://doi.org/10.24963/ijcai.2021/610). URL <https://doi.org/10.24963/ijcai.2021/610>. Survey Track.

Kraul, S., Seizinger, M., and Brunner, J. O. Machine learning-supported prediction of dual variables for the cutting stock problem with an application in stabilized column generation. *INFORMS Journal on Computing*, 35(3):692–709, 2023. doi: [10.1287/ijoc.2023.1277](https://doi.org/10.1287/ijoc.2023.1277).

Lubin, M., Yamangil, E., Bent, R., and Vielma, J. P. Extended Formulations in Mixed-Integer Convex Programming. In Louveaux, Q. and Skutella, M. (eds.), *Proceedings of the 18th Conference on Integer Programming and Combinatorial Optimization (IPCO 2016)*, volume

9682 of *Lecture Notes in Computer Science*, pp. 102–113, 2016.

Mak, T. W., Chatzos, M., Tanneau, M., and Van Hentenryck, P. Learning regionally decentralized ac optimal power flows with admm. *IEEE Transactions on Smart Grid*, 14(6):4863–4876, 2023.

MOSEK Aps. *The MOSEK optimization toolbox for Julia manual. Version 10.1.23.*, 2023a. URL <https://docs.mosek.com/latest/juliaapi/index.html>.

MOSEK Aps. *The MOSEK Modeling Cookbook*, 2023b. URL <https://docs.mosek.com/modeling-cookbook/index.html>.

Pan, X., Zhao, T., Chen, M., and Zhang, S. Deepopf: A deep neural network approach for security-constrained dc optimal power flow. *IEEE Transactions on Power Systems*, 36(3):1725–1735, 2020.

Parikh, N., Boyd, S., et al. Proximal algorithms. *Foundations and trends® in Optimization*, 1(3):127–239, 2014.

Park, S. and Van Hentenryck, P. Self-supervised primal-dual learning for constrained optimization. In *Proceedings of the AAAI Conference on Artificial Intelligence*, volume 37, pp. 4052–4060, 2023.

Qian, C., Chételat, D., and Morris, C. Exploring the power of graph neural networks in solving linear optimization problems. *arXiv preprint arXiv:2310.10603*, 2023. URL <https://doi.org/10.48550/arXiv.2310.10603>.

Qiu, G., Tanneau, M., and Hentenryck, P. V. Dual conic proxies for ac optimal power flow, 2023.

Santos Xavier, A., Qiu, F., Gu, X., Becu, B., and Dey, S. S. MIPLearn: An Extensible Framework for Learning-Enhanced Optimization, June 2023.

Sugishita, N., Grotthey, A., and McKinnon, K. Use of machine learning models to warmstart column generation for unit commitment, 2023.

Tordesillas, J., How, J. P., and Hutter, M. Rayen: Imposition of hard convex constraints on neural networks. *arXiv preprint arXiv:2307.08336*, 2023.

Ziegler, H. Solving certain singly constrained convex optimization problems in production planning. *Operations Research Letters*, 1(6):246–252, 1982. ISSN 0167-6377. doi: 10.1016/0167-6377(82)90030-X.

A. Experiment Details

All experiments are conducted on Intel Xeon Gold 6226 CPU @ 2.70GHz nodes, using a single Tesla V100 GPU; each job was allocated 12 CPU threads and 64GB of RAM. All ML models are formulated and trained using Flux (Innes et al., 2018), with (sub)gradients computed using the auto-differentiation backend Zygote (Innes, 2018). All linear and mixed-integer problems are solved with Gurobi v10 (Gurobi Optimization, 2018). All nonlinear conic problems are solved with Mosek (MOSEK Aps, 2023a). Detailed experimental settings, such as data-generation procedures, model architectures, and hyper-parameters are provided below.

A.1. Multi-Dimensional Knapsack

For each number of items $n \in \{100, 200, 500\}$ and number of resources $m \in \{5, 10, 30\}$, 16384 instances are generated using the same procedure as the MIPLearn library (Santos Xavier et al., 2023). Each instance is solved with Gurobi, and the optimal dual solution is recorded for evaluation purposes. This dataset is split in training, validation and testing sets, which contain 8192, 4096 and 4096 instances, respectively.

The architecture considered here is a fully-connected neural network (FCNN); a separate model is trained for each combination (m, n) . The FCNN model takes as input the flattened problem data (b, p, W) , and outputs $y \in \mathbb{R}^m$. The FCNN has two hidden layers of size $2(m + n)$ and sigmoid activation; the output layer uses a negated softplus activation to ensure $y \leq 0$.

The models are trained in a self-supervised fashion, by maximizing the Lagrangian function $\mathcal{L}(y)$ defined in (39). The experiments use the Adam optimizer with a learning rate of 10^{-5} , kept constant throughout training. Each model is trained for up to 512 epochs; the model with the best validation loss is selected and evaluated on the test set. This choice of hyper-parameters was found to achieve satisfactory performance for the case at hand. The use of graph neural network (GNN) architectures, which would support arbitrary numbers of items and resources, is a promising avenue for future research; a systematic comparison of the performance of GNN and FCNN architectures is, however, beyond the scope of this work.

A.2. Production and Inventory Planning

For each $n \in \{10, 20, 50, 100, 200, 500, 1000\}$, 16384 instances are generated using the procedure of (Ziegler, 1982). First, D_j is sampled from a uniform distribution $U[1, 100]$, c_j^p is sampled from $U[1, 10]$, and c_j^r is sampled from $U[0.05, 0.2]$. Then, $c_j^o = \alpha_j c_j^p$ and $r_j \sim \beta_j c_j^p$, where α, β are sampled from $U[0.1, 1.5]$ and $U[0.1, 2]$, respec-

tively. Finally, the right-hand side is $b = \eta \sum_j r_j$ where η is sampled from $U[0.25, 0.75]$. The lower and upper bounds on variables x, t are then computed following (42).

Each instance is solved with Mosek, and its solution is recorded for evaluation purposes. The dataset is split into training, validation and testing sets comprising 8192, 4096 and 4096 instances, respectively.

The paper considers FCNN models that take as input $(d, f, r, b) \in \mathbb{R}^{1+3n}$, and output $(\bar{y}, \bar{\pi}, \bar{\tau}, \bar{\sigma}) \in \mathbb{R}^{1+3n}$. The models have two hidden layers of size $4n$. When using the bounded formulation (43), the output of the last hidden layer is then passed to four independent, fully-connected layers that output $\bar{y}, \bar{\pi}, \bar{\tau}, \bar{\sigma}$, respectively. A negated softplus activation ensures $\bar{y} \leq 0$, softplus activations ensures $\bar{\pi}, \bar{\tau} > 0$, and σ is unrestricted. The solution $(\bar{\pi}, \bar{\tau}, \bar{\sigma})$ is then projected onto a conic-feasible $(\hat{\pi}, \hat{\tau}, \hat{\sigma})$. When using the original formulation (41), only the output \bar{y} is kept, followed by the closed-form dual completion procedure outlined in Section 5.2.2.

All models are trained in a self-supervised fashion using the proposed DLL methodology. For the bounded formulation, the training maximizes the Lagrangian $\mathcal{L}(\hat{y}, \hat{\pi}, \hat{\tau}, \hat{\sigma})$ in (45). For the original formulation, the training maximizes the Lagrangian $\tilde{\mathcal{L}}(\hat{y})$ in (47). Note that both settings use the same underlying architecture, data, weight initialization, and other hyper-parameters, i.e., only the training loss differs. All models are trained using the Adam optimizer with learning rate 10^{-4} , for up to 4096 epochs. The model with best validation loss is selected and evaluated on the test set.

It is important to note that, when considering the bounded formulation, two valid Lagrangian bounds can be derived from a prediction $(\hat{y}, \hat{\pi}, \hat{\tau}, \hat{\sigma})$. On the one hand, one can directly compute $\mathcal{L}(\hat{y}, \hat{\pi}, \hat{\tau}, \hat{\sigma})$: this is the approach used to compute the training loss. On the other hand, one may discard $(\hat{\pi}, \hat{\tau}, \hat{\sigma})$ and instead compute $\tilde{\mathcal{L}}(\hat{y})$. Experimental results have shown that the latter approach provides significantly better bounds, i.e., the authors have observed that $\mathcal{L}(\hat{y}, \hat{\pi}, \hat{\tau}, \hat{\sigma}) \ll \tilde{\mathcal{L}}(\hat{y})$. Therefore, to ensure a fair comparison, both approaches (bounded and original formulations) are evaluated on the test set using the same Lagrangian function $\tilde{\mathcal{L}}$. In addition, when training dual proxies under the bounded formulation, the best model is selected according to $\tilde{\mathcal{L}}$. Thus, the Lagrangian function \mathcal{L} is only used to compute the training loss and evaluate gradients.